

Harmonic assessment on two photovoltaic inverter modes and mathematical models on low voltage network power quality

Ontoseno Penangsang, Rony Seto Wibowo, Ni Ketut Aryani, Mario Dwi Prasetyo,
Marcel Nicky Arianto, Aulia Amjad Lutfi

Department of Electrical Engineering, Faculty of Intelligent Electrical and Informatics Technology, Institute of Technology Sepuluh Nopember, Surabaya, Indonesia

Article Info

Article history:

Received Oct 21, 2022

Revised Feb 6, 2023

Accepted Mar 9, 2023

Keywords:

Harmonics

Inverter

Photovoltaic

Power factor

Total harmonic distortion

ABSTRACT

Power quality is a crucial aspect of designing a large-scale photovoltaic power plant, particularly regarding harmonics caused by inverter switching. This research aimed to analyze harmonics in a system using electrical transient analyzer program (ETAP) Power Station 20.5.0 to uncover the effect of irradiance on the inverters' power quality running at 85% and 100% power factors. We analyzed both voltage and current total harmonic distortion (THD_i and THD_v) from the simulation and compared them with the mathematical model. Moreover, we analyzed the effect of changes in irradiance level on harmonics and reactive power penetration, which influenced power losses in transformers and cables. Inverters at 85% power factor experienced an increase in THD_i , whereas those at 100% power factor decreased. Inverters with 85% power factor experienced more frequent switching, causing more prominent distortion. The magnitude of THD_v increased proportionally with the rise of irradiance level. Inverters at 85% had a higher THD_v value because of the excessive reactive power compensation when irradiance rose. Irradiance level had an inverse relationship with system losses since high irradiance levels led to lower losses as less power was required through transmission lines and transformers. Moreover, losses at 85% power factor were higher since the high harmonics caused additional losses.

This is an open access article under the [CC BY-SA](https://creativecommons.org/licenses/by-sa/4.0/) license.



Corresponding Author:

Ontoseno Penangsang

Department of Electrical Engineering, Faculty of Intelligent Electrical and Informatics Technology,

Institute of Technology Sepuluh Nopember

Surabaya, Indonesia

Email: zenno379@gmail.com

1. INTRODUCTION

An interconnected or grid-tied photovoltaics (PV) system must fulfill specific criteria like voltage level, phase sequence, and frequency, as stated in the IEEE standard of distributed energy resources (DER) [1]. In order to satisfy those standards, power electronics technology is needed to increase energy conversion efficiency and reliability and to reduce cost. An inverted-connected PV system has several essential features, such as maximum power point tracking, anti-islanding, grid fault detection, and many others [2]. An inverter controls its switch using sequential sinusoidal control voltage to change the DC voltage from renewable energy sources to the 3-phase AC voltage needed by the electricity network [3]. An inverter can be operated as power electronics equipment for renewable energy sources such as grid-connected PV [4]. Inverter is categorized as a non-linear load if its output value is not proportional to the input voltage [5]. However, the intermittent nature of solar energy and the operation characteristics of inverters in PV systems can cause adverse effects such as protection coordination failure, high conductor losses, voltage fluctuation, harmonic distortion, and grid disturbance [6].

The inverter's output voltage should be a sine wave. In practice, the output voltage is non-sinusoidal and contains harmonics [7]. The assessment of the non-sinusoidal waveform can be done using Fourier transformation [8]. So, harmonic distortion became a severe issue in new renewable energy utilization. If the harmonic distortion problem is not solved, further renewable energy penetration cannot reach its full potential [9]. Harmonics affects the distribution networks by increasing the heating losses and decreasing the operation life of insulations [10]. Based on Germany's standard of voltage regulation VDE-AR-N 4105, inverters must supply their load with reactive power [11]. The inverter's capability to generate reactive power depends on the active power supplied by the PV arrays. Grady and Gilleskie [12] in Elkholy's [2] paper also researched the effect of harmonics on power factors (PFs). They created a mathematical model called true power factor (TPF) [2]. TPF can be implemented in harmonics analysis to limit the harmonics caused by nonlinear load using the widely accepted concept of power factor.

Past research has discussed photovoltaics' operation on low voltage networks and quality assessment on inverter power output. Elkholy's research [2] on harmonics assessment on low voltage networks in Electronic Research Institute Building, Cairo, is the primary reference for our research. The data used in that research was extracted directly from the building's electrical system within a specified time range, then compared using mathematical analysis of power factor and total harmonic distortion (THD) [2]. Another relevant research was done by Rampinelli *et al.* [13] using direct measurement in the Solar Energy Laboratory of Federal University Rio Grande do Sul and mathematical model simulation using ten models of inverters [13]. Both of those researchers analyzed the characteristics of THD of on-field inverters with power factor setting as the treatment variables. However, they have yet to discuss the effect of different power factor setting on the system.

Our research adds a new perspective by simulating the system using electrical transient analyzer program (ETAP) 20.5.0 software. This software analyzes the effect of irradiance on the inverter's power quality while operating at 85% and 100% power factor. From the simulation result, we look into the total current and voltage harmonic distortion (THD_i and THD_v), then compare them with values based on mathematical analysis. We also analyze the effect of PV penetration at every inverter power level on harmonics-induced transformer and system losses. This research can predict the condition and effect of harmonics in PV-integrated systems on 100% or 85% power factor under every irradiance level.

2. METHOD

This research is conducted by performing simulations in ETAP Power Station 20.5.0 software to analyze harmonics. ETAP 20.5.0 is widely used for power system simulation since it is commercial software for simulating and designing electrical power systems in industries and academics. Moreover, ETAP Power Station has a comprehensive interface and can be run on Windows operating system, making it an excellent analysis tool for designing and testing the power system. ETAP can be used in offline mode for real-time monitoring, simulation, optimization, energy management system, and high-speed intelligent loading with real-time data operation [14]. Our research follows a workflow, as shown in Figure 1.

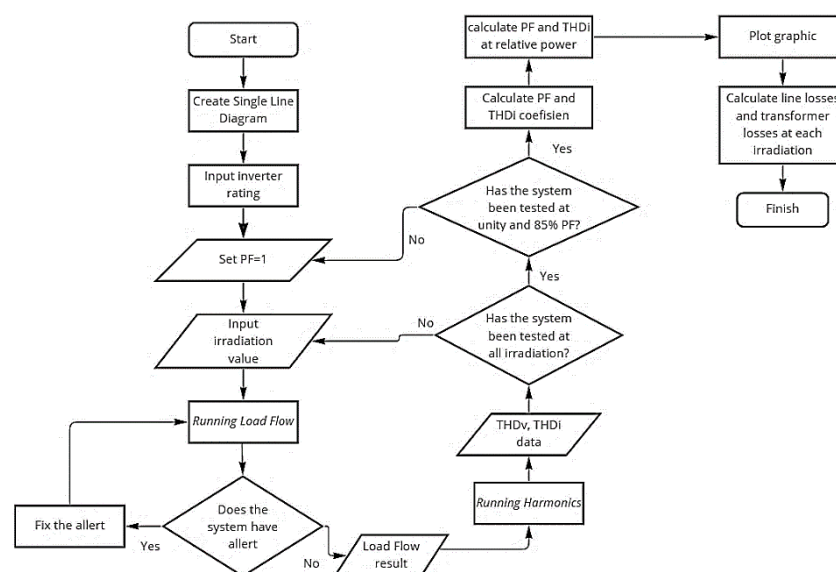


Figure 1. Research flowchart

2.1. System

The power system network used for the simulation came from Bhatt’s [15] research, with several adjustments. In this system, there are six individual PV arrays, four lump load, and two static load that is supplied by the grid as shown in Figure 2. However, the irradiance data is only simulated on 0.4 kV PVs: PV A1, PV A2, PV A3, and PV A4. The rest of the PV arrays, PV A5 and PV A6, are connected to 6.3 kV busses and supply Load 1 and Load 2 with constant power. The PV and inverter ratings in every PV array are shown in Table 1. Simulation is performed on PV A1 through PV A4 by using irradiance data of Surabaya city, as shown in Table 2. The data given below can be fully accessed from the Global Solar Atlas website. Each average irradiance data will be applied to every low-voltage PV inverter on two different power factor levels, 100% and 85%.

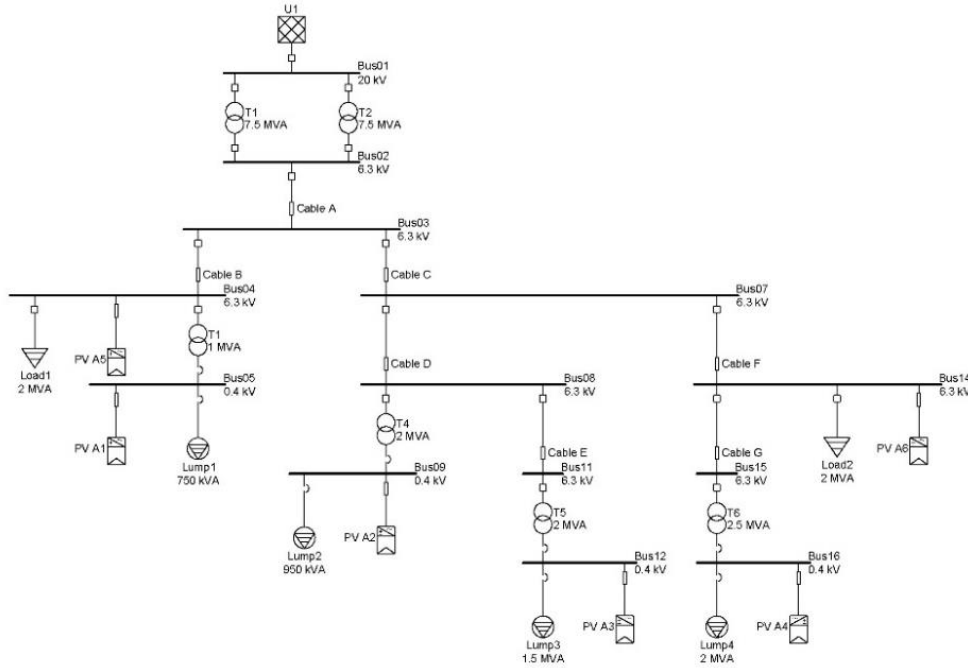


Figure 2. Single line diagram of system

Table 1. PV and inverter rating

PV array	PV array rating			DC inverter rating			AC inverter rating	
	V _{DC} (Volts)	I _{DC} (A)	P _{DC} (kW)	P _{DC} (kW)	V _{DC} (kV)	Eff (%)	S (kVA)	V _{AC} (kV)
PV A1	1031.7	714.4	692.422	833.3	0.4	90	750	0.4
PV A2	1031.7	899	871.36	1111.1	0.4	90	1,000	0.4
PV A3	1024.9	1383.9	1350.9	1642.1	0.4	90	1,560	0.4
PV A4	1497.2	1862.9	1244.25	2333.3	0.4	90	2,100	0.4
PV A5	3801.2	1998.1	525.64	2105.3	11	95	2,000	6.3
PV A6	3837	2046.9	533.37	2222.2	11	95	2,000	6.3

Table 2. Solar irradiance data

Hour	Solar irradiance (W/m ²)												
	Jan	Feb	Mar	Apr	May	Jun	Jul	Aug	Sept	Oct	Nov	Dec	Average
7-8	150	125	151	187	211	225	208	265	345	293	226	140	210
8-9	229	235	290	310	362	380	425	468	515	446	335	221	351
9-10	308	319	359	389	460	473	531	587	632	555	405	292	442
10-11	358	357	409	466	532	543	614	679	707	629	468	335	508
11-12	357	380	453	523	595	594	670	737	751	658	497	345	547
12-13	335	357	442	526	603	619	686	754	749	642	460	317	541
13-14	296	331	395	456	564	606	672	736	721	595	377	252	500
14-15	245	281	307	349	484	546	625	688	654	481	287	193	428
15-16	167	194	215	247	364	445	540	589	545	392	201	123	335
16-17	109	133	139	175	256	340	416	450	409	281	145	79	244
17-18	84	93	97	109	117	183	235	266	230	143	86	54	142
Average value in a day													377

2.2. Harmonics simulation using ETAP

Simulation using ETAP is divided into fundamental power flow simulation and harmonic power flow. In the fundamental simulation, the system will be tested for every change in irradiance as shown in Table 2 for each power factor change of 1 and 0.85. The observed results are changes in power flow, current in each line, and voltage at each busbar. Meanwhile, harmonic load flow analysis will be conducted to observe changes in each fundamental condition, such as changes in current and voltage under harmonic conditions. These current and voltage values are represented in root mean square (RMS) values. The RMS values depend on the characteristics of harmonic distortion at each measurement point. As shown in (1) and (2) represent the relationship between RMS values of current and voltage with harmonics [16].

$$V_{rms} = V_1 \sqrt{1 + \left(\frac{THD_v}{100}\right)^2} = V_1 \sqrt{1 + (THD_{v_{pu}})^2} \quad (1)$$

$$I_{rms} = I_1 \sqrt{1 + \left(\frac{THD_i}{100}\right)^2} = I_1 \sqrt{1 + (THD_{i_{pu}})^2} \quad (2)$$

The magnitude of total harmonic distortion of current (THD_i) and total harmonic distortion of voltage (THD_v) is determined through (3) to (4) [17]. THD_i value is a primary characteristic used to analyze the level of harmonics in an inverter. On the other hand, THD_v represents the distortion caused by the injection of distorted current through an impedance [18].

$$THD_v = \frac{\sqrt{\sum_{n=2}^n \max V_n^2}}{V_1} \quad (3)$$

$$THD_i = \frac{\sqrt{\sum_{n=2}^n \max I_n^2}}{I_1} \quad (4)$$

Harmonic load flow analysis is also performed to obtain changes in power factor due to harmonic distortion, known as the TPF. TPF is the ratio of real power output to the apparent power output of the circuit. It is typically viewed as the amount of power that could be consumed by the load [12]. The TPF is modeled as (5):

$$TPF = \frac{P_{avg}}{V_{1\ rms} I_{1\ rms}} \cdot \frac{1}{\sqrt{1 + \left(\frac{THD_i}{100}\right)^2}} \quad (5)$$

where, $\frac{1}{\sqrt{1 + \left(\frac{THD_i}{100}\right)^2}}$ is a distortion factor (DF). Meanwhile $\frac{P_{avg}}{V_{1\ rms} I_{1\ rms}}$ is a displacement power factor (DPF) that also represented as $\cos\theta_{vi}$. So, the value of TPF can also be expressed as (6) [12].

$$pf_{true} = DF \cdot \cos\theta_{vi} \quad (6)$$

2.3. Modelling true power factor and THD_i using MATLAB

Simulation results from ETAP Power Station will give us each inverter's characteristics and power quality at a given irradiance level. Then, those data will be processed in MATLAB R2021B to find all variables in the mathematical model for power factor and THD_i parameters. Those equations are needed to find the characteristic of each inverter.

Equations (1) to (6) show the modeled calculation for TPF and THD_i but neglected the effect of irradiance on the true power factor, whereas irradiance and the output of the inverter affect the TPF. Hence, a mathematical model is needed to calculate the true power factor on an inverter's varying output power towards its irradiance (through the ratio of P_{AC} and P_{NOM}) [13]. Equation suitable for the mathematical model for calculating the average value of power factor on different load conditions are expressed by (7).

$$pf = \frac{C_0 \cdot C_1 + (C_2 \cdot (P_{AC}/P_{NOM})^{C_3})}{C_1 + (P_{AC}/P_{NOM})^{C_3}} \quad (7)$$

Coefficients C_0 , C_1 , C_2 , and C_3 are obtained by applying the measured curve in MATLAB. The ratio of P_{AC} and P_{NOM} indicates the output efficiency of the inverter. Equation suitable for the mathematical model for calculating the average value of power factor on different load conditions are expressed by (8).

$$THD_i = T_0 \cdot \exp(-T_1(P_{AC}/P_{NOM})) + T_2 \cdot \exp(-T_3(P_{AC}/P_{NOM})) \quad (8)$$

Coefficients T_0 , T_1 , T_2 , and T_3 are obtained by applying the measured curve. The ratio of P_{AC} and P_{NOM} indicates the output efficiency of the inverter.

2.4. Harmonics impact analysis

After the condition in the previous analysis, we will continue by doing a harmonics analysis to determine the amount of harmonics-induced transformer and system power losses. These losses are calculated for 100% and 85% power factor for every irradiance level. The rating of each transformer in the system is shown in Table 3. The IEC-60076 standard is used as a reference for the calculation of no-load and on-load losses. The rating for the electric lines is shown in Table 4.

Table 3. Transformer rating

Transformer ID	Capacity (MVA)	High voltage side (kV)	Low voltage side (kV)	Impedance (%)	No-Load losses (kW)	On-Load losses (kW)
T1	7.5	20	6.3	8.35	7	46
T2	7.5	20	6.3	8.35	7	46
T3	1	6.3	0.4	5	1.95	12
T4	2	6.3	0.4	5.7	2.7	25
T5	2	6.3	0.4	5.7	2.7	25
T6	2.5	6.3	0.4	6.25	2.8	28

Table 4. Cable rating

Cable ID	From Bus	To Bus	Length (m)	Impedance (Ω/m)
Cable A	Bus 02	Bus 03	100	0.08387
Cable B	Bus 03	Bus 04	100	0.35434
Cable C	Bus 03	Bus 07	50	0.02695
Cable D	Bus 07	Bus 08	50	0.2695
Cable E	Bus 08	Bus 11	50	0.01771
Cable F	Bus 07	Bus 14	50	0.02695
Cable G	Bus 14	Bus 15	50	0.02695

Transformer power loss caused by harmonics can be classified into on-load loss and no-load loss. The total power loss in transformers can be modeled as shown in (9). In the equation, P_{TL} is the transformer's total losses, P_{NL} is the no-load transformer losses, and P_{LL} is the on-load transformer losses. In a no-load transformer, the losses produced by the transformer are not affected by harmonics. The total losses caused by the harmonics can be calculated using (10) (using per-unit system).

$$P_{TL} = P_{NL} + P_{LL} \quad (9)$$

$$P_{LL-R}(pu) = P_{I^2R-R} + [(F_{HL} \times P_{EC}) + (F_{HL-STR} \times P_{OSL})] \quad (10)$$

where P_{LL} is the total losses of an on-load transformer caused by harmonics, PP_{I^2R-R} is the DC I²R harmonics losses, F_{HL} is the harmonics factor for eddy current losses on the transformer's winding, P_{EC} is the eddy current losses on the transformer's winding. The eddy current losses will cause excessive core losses and abnormal temperature changes in the transformer [4]. F_{HL-STR} is the loss factor caused by harmonics current on other stray losses, and P_{OSL} is the stray losses.

Loss analysis in transformers and lines requires calculations to determine the impedance values. This is because the available ratings are still in per-unit values with a base of 100 kVA. To determine the ohmic value of resistance (R), reactance (X), and impedance (Z) of the transformer, equations (11) to (12) are used [19].

$$Z_{base,pu} = \frac{kV^2}{MVA} \quad (11)$$

$$X_{pu} = \frac{Z_{base}}{100} \cdot \sin(\tan^{-1}[\frac{X_{pu}}{R_{pu}}]) \quad (12)$$

$$R_{pu} = \frac{\%Z_1}{100} \cdot \cos(\tan^{-1}[\frac{X_{pu}}{R_{pu}}]) \quad (13)$$

3. RESULTS AND DISCUSSION

3.1. Effect of harmonics

The simulation was done in ETAP Power Station to determine the effect of solar power plant installation with the different inverter operation modes. The result of the simulation will give the power and harmonics data in a distribution network. Each of the average irradiance levels in Table 2 is used as the independent variable, with the inverters' power output and quality as the dependent variable. The database used for harmonics simulation can be seen in Table 5.

The result of the simulation in Table 5 is processed using line charts to understand better the effect of irradiance on the change of active and reactive power in each inverter operation mode. As shown in Figure 3, it can be inferred that the higher the irradiance, the higher the active power generated by the inverter while working under 100% power factor in Figure 3(a) and 85% power factor in Figure 3(b). Inverters working in power factors produce the same active power because the inverter's type stays the same. Reactive power produced by the inverters is proportional to the irradiance received by the PV arrays [20]. Inverters with a 100% power factor produce no reactive power because they only generate active power. Inverters with an 85% power factor produce reactive power proportional to their active power, with an active-reactive ratio dictated by the power factor. In past research, active and reactive power generated by inverters can be controlled to match the demand. One of the methods to achieve such control is by controlling the reactive power output to mitigate voltage sag in the system [21].

Table 5. Harmonics simulation data at each irradiance level

Irradiance (W/m ²)	P (kW)	Unity power factor				85% power factor			
		Q(kvar)	THD _i (%)	THD _v (%)	Power Factor	Q(kvar)	THD _i (%)	THD _v (%)	PF
142	0.014	0	48614	4.66	0.002	0.008	41286	4.66	0.002
210	0.024	0	27163	4.66	0.004	0.015	23053	4.66	0.004
244	0.061	0	10895	4.66	0.009	0.038	9225.4	4.66	0.009
300	0.288	0	2310	4.65	0.043	0.179	1936	4.67	0.044
330	194.3	0	30.37	5.15	0.957	120.4	25.76	7.39	0.823
335	197.5	0	30.27	5.22	0.957	122.4	25.73	7.55	0.823
351	207.5	0	30.09	5.36	0.958	128.6	25.75	7.84	0.823
428	256.4	0	29.68	5.93	0.959	158.9	26.1	8.66	0.822
442	265.4	0	29.62	6.04	0.959	164.5	26.16	8.81	0.822
500	302.7	0	29.42	6.53	0.959	187.6	26.33	9.44	0.822
508	307.8	0	29.39	6.6	0.959	190.8	26.35	9.52	0.822
541	329.2	0	29.3	6.9	0.960	204	26.44	9.88	0.822
547	333.1	0	29.29	6.95	0.960	206.4	26.45	9.94	0.822

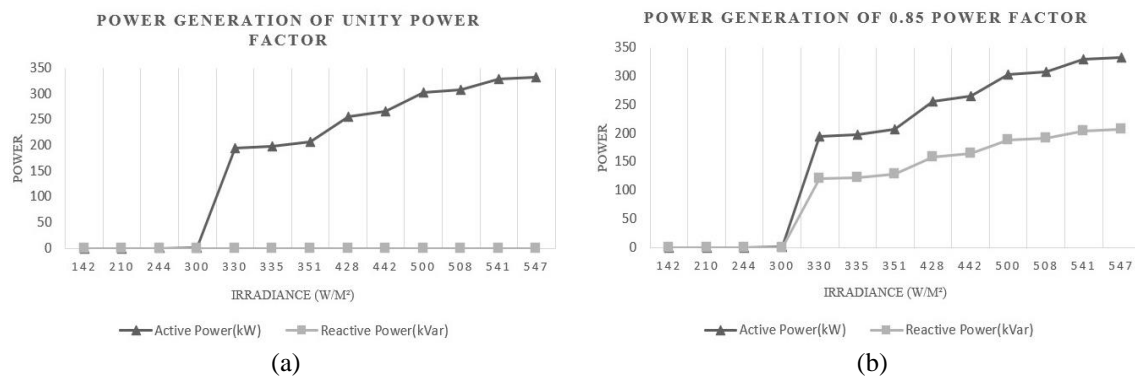


Figure 3. Comparison of active and reactive power at all irradiance levels (a) 100% PF and (b) 85% PF

Irradiance's effect on the system's harmonics can be observed by looking at the magnitude of THD_i and THD_v. THD_i and THD_v data are extracted when the inverter works below its nominal power. This is done because THD_i data is difficult to observe when inverters are operating at their nominal power [22]. From Figure 4, it can be inferred that the larger the irradiance, the smaller the THD_i in the system, regardless of whether the inverter is working on 100% PF in Figure 4(a) or 85% PF in Figure 4(b). Therefore, it can be concluded that the value of THD_i is affected by the active power output of the inverters. The value of THD_i is very large at an irradiance level below 330 W/m². This is caused by the high harmonics current when inverters work less than 20% of their nominal power [23]. In this case, the inverter's nominal power is 714.4 kW, which

means 330 W/m^2 is the threshold where they generate more than 20% of the nominal active power. Inverters in 100% power factor have a slightly smaller THD_i value than those in 85% power factor.

Analysis of the effect of irradiance on THD_v shows that both parameters are proportional to each other, as shown in Figure 5. That applies to both 100% power factor shown in Figure 5(a) and 85% power factor shown in Figure 5(b). This characteristic is opposite to THD_i , where irradiance is inversely proportional to THD_i [24].

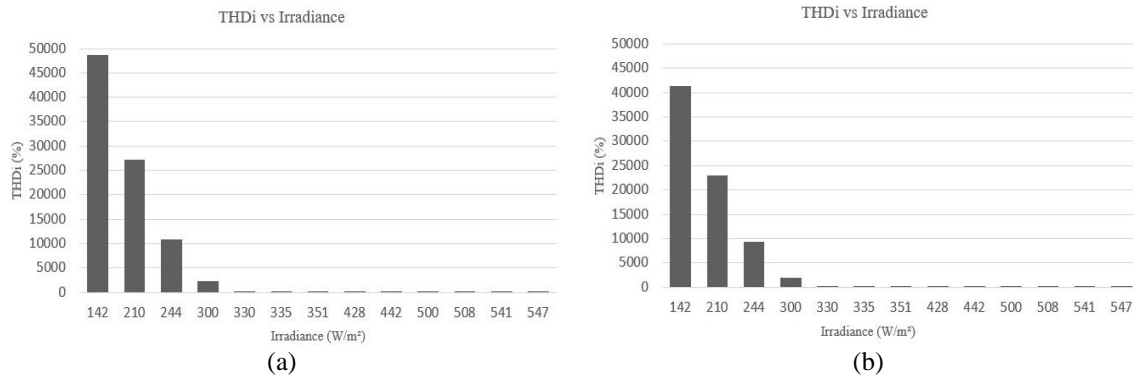


Figure 4. Comparison of THD_i at all irradiance levels (a) 100% PF and (b) 85% PF

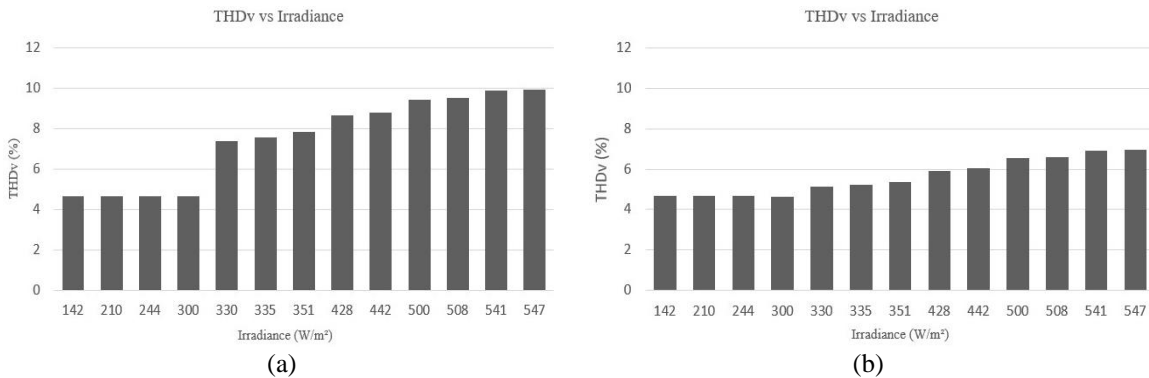


Figure 5. Comparison of THD_v at all irradiance levels (a) 100% PF and (b) 85% PF

Inverters will try to match their generation power factor with the setting power factor. If it is set at 100% power factor, then the generation power factor will not necessarily be exactly 100%, but there will be a slight deviation. The same thing applies to the 85% power factor. As shown in Figure 6, when irradiance is at 330 W/m^2 , there is a drastic increase in power generated compared to when irradiance is at 300 W/m^2 at 100% PF as shown in Figure 6(a) and 85% PF as shown in Figure 6(b). This happens because, at an irradiance level of 300 W/m^2 and below, PV arrays' output current and voltage do not fulfill the minimum voltage level for MPPT in inverters to activate. Therefore, the output power will be minimal. If compared between both operation modes, inverters working at 85% generate smaller THD_i or harmonics current compared to ones working at 100%. Inverters with a 100% power factor tend to absorb reactive power, making the THD_i value slightly larger [22].

3.2. Simulation result of ETAP Power Station

Figure 7 shows a comparison between output active power characteristics and relative power characteristics (P_{AC}/P_{NOM}) with the inverter's generation power factor at 100% PF and 85% PF for inverter PV A1 as shown in Figure 7(a), PV A2 as shown in Figure 7(b), PV A3 as shown in Figure 7(c), and PV A4 as shown in Figure 7(d). In order to obtain a viable result, this research compared the mathematical calculation result with the ETAP Simulation. Figure 7 also represents the difference between ETAP Power Station simulation and mathematical calculation. The coefficient used to model the inverter's characteristics using mathematical calculation is acquired using (4) and the result is shown in Table 6.

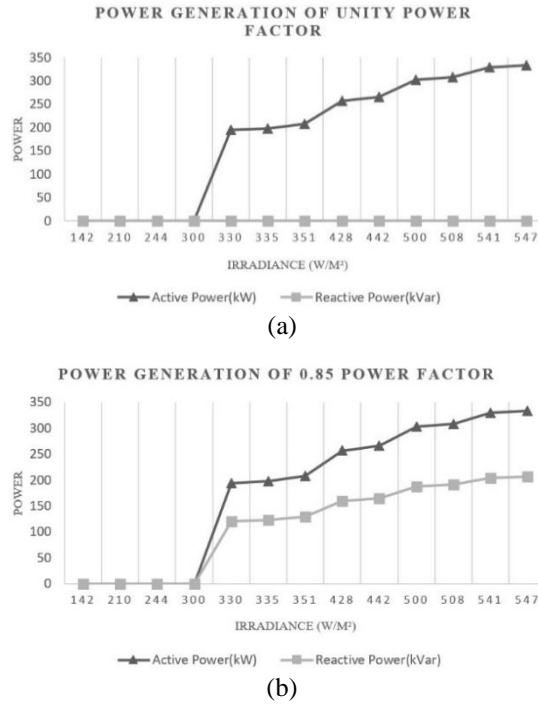


Figure 6. Comparison of power factor at all irradiance levels (a) 100% PF and (b) 85% PF

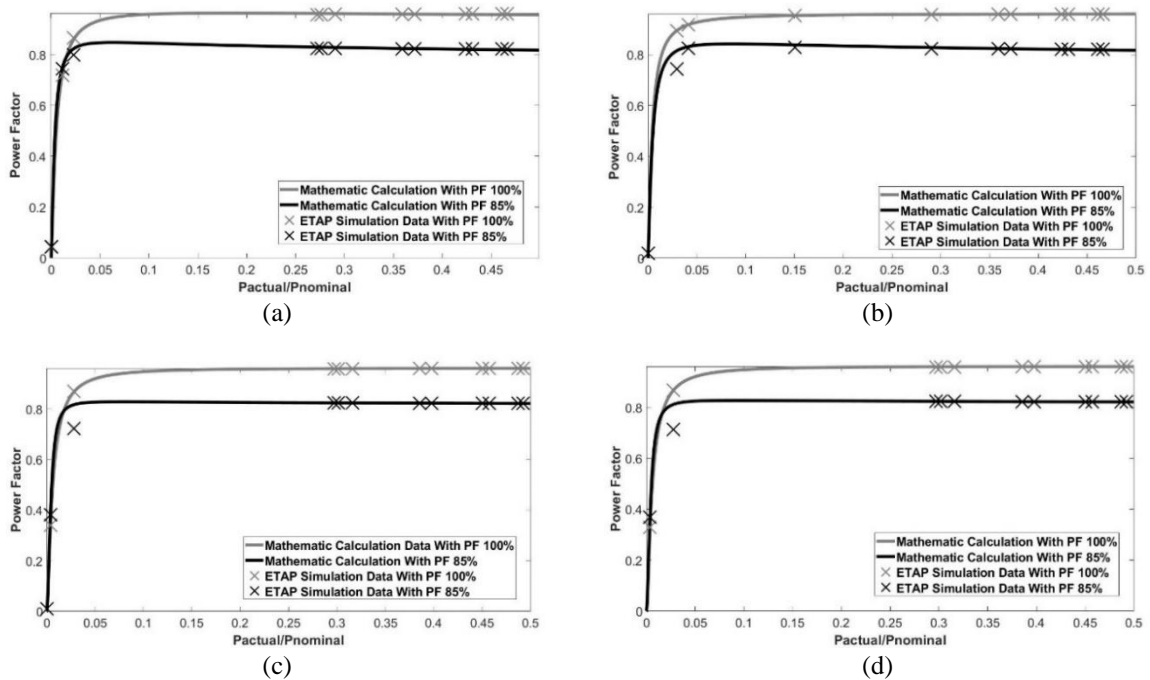


Figure 7. Inverter's power factor comparison between data from simulation and mathematical calculation (a) PV A1, (b) PV A2, (c) PV A3, and (d) PV A4

The generation power factor is relatively constant when the inverters are working at around 5% of relative power and above. That pattern applies to both 85% and 100% power factors. The data trends acquired from ETAP Simulation and mathematical calculation have the same pattern. If Figure 7 is compared with Figure 8 for inverter PV A1 as shown in Figure 8(a), PV A2 as shown in Figure 8(b), PV A3 as shown in Figure 8(c), and PV A4 as shown in Figure 8(d), it will show that the higher the relative power, the closer the

power factor to 100% with a smaller THD_i [23]. Therefore, we can analyze the relative power of past research. Rampinelli *et al.* [13] analyzed the characteristics of IG 30 inverters with 100% and 95% power factors. The comparison of the power factor in this research and past research is shown in Table 7.

Table 6. Mathematical power factor coefficient

PV title	100% power factor				85% power factor			
	C ₀	C ₁	C ₂	C ₃	C ₀	C ₁	C ₂	C ₃
PV A1	0.9481	1.211	0.001715	1.228	0.8031	1.369	0.000398	1.395
PV A2	0.9607	1.294	0.0008169	1.295	0.8028	1.29	0.0008401	1.318
PV A3	0.9596	1.387	0.0008299	1.39	0.8177	1.992	0.000185	1.998
PV A4	0.9604	1.391	0.0008016	1.394	0.8184	1.869	0.00003603	1.875

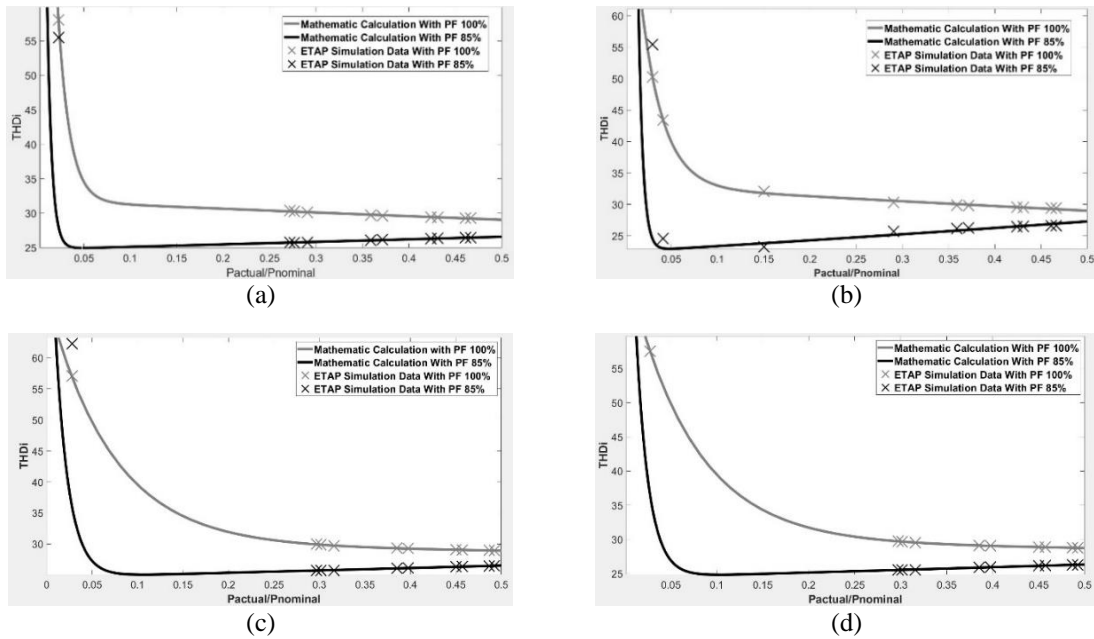


Figure 8. Comparison of THD_i characteristics in each inverter (a) PV A1, (b) PV A2, (c) PV A3, and (d) PV A4

Table 7. Actual power factor at several relative power operations

Inverter ID	Operation mode	Actual power factor at % of relative power						
		0.5%	5%	10%	20%	30%	40%	50%
IG 30	Unity PF	-	0.237783	0.944954	0.958365	0.959607	0.959756	0.959792
	95% PF	-	0.6132	0.9425	0.95845	0.95957	0.95976	0.95979
PV A1	Unity PF	0.483	0.922	0.946	0.956	0.958	0.960	0.960
	85% PF	0.617	0.818	0.822	0.824	0.824	0.824	0.824
PV A2	Unity PF	0.539	0.926	0.947	0.955	0.958	0.959	0.959
	85% PF	0.086	0.822	0.823	0.823	0.823	0.823	0.823
PV A3	Unity PF	0.424	0.919	0.945	0.956	0.959	0.960	0.960
	85% PF	0.491	0.818	0.821	0.822	0.822	0.822	0.822
PV A4	Unity PF	0.426	0.919	0.946	0.956	0.959	0.960	0.961
	85% PF	0.487	0.817	0.821	0.823	0.823	0.823	0.823

The coefficient that determines the inverters' characteristics from the relation between P_{AC}/P_{NOM} and THD_i is shown in Table 8. Based on the coefficients in Table 8, we can compare the P_{AC}/P_{NOM} data acquired from ETAP and mathematical calculation to identify the characteristics of an inverter when connected to the system. While Figure 7 shows the relation between P_{AC}/P_{NOM} and THD_i, Figure 8 compares the THD_i characteristic curve of each inverter in the system.

Figure 8 shows that THD_i at 100% power factor is more prominent than at 85%. This confirms the true power factor principle, where THD_i is affected by the power factor [25]. The relationship between THD_i and the power factor is proportional: the more significant the power factor, the bigger the THD_i. Therefore, THD_i is bigger when inverters are operating at 100%. When relative power is less than 5%, the magnitude of

THD_i is enormous. When the relative power is above 5%, inverters operating on 85% power factor tend to increase, while ones on 100% power factor decrease. The increase and decrease in THD_i are not significant.

The THD_i value at several relative power can be seen in Table 9. Those data are acquired from the mathematical calculation, with coefficients achieved using the curve fitting method in Table 8. The result of this calculation is compared with the data acquired from the research done by Rampinelli *et al.* [13] on IG 30 inverters. It is worth noting that Rampinelli did an on-field measurement on inverters operating at 10% of relative power with 100% and 95% power factors.

Table 8. THD_i coefficient

PV Title	100% power factor				85% power factor			
	T ₀	T ₁	T ₂	T ₃	T ₀	T ₁	T ₂	T ₃
PV A1	31.76	0.1791	160.2	78.99	293.7	198.5	24.76	-0.1421
PV A2	32.92	0.2538	61.7	42.21	757.2	202.9	22.47	-0.3891
PV A3	29.92	0.06948	40.02	14.02	77.34	68.76	24.62	-0.1486
PV A4	29.72	0.06953	41.13	14.19	87.33	72.21	24.39	-0.1531

Table 9. THD_i magnitude at several relative power operations

Inverter ID	Operation mode	THD _i magnitude at % of relative power						
		0.5%	5%	10%	20%	30%	40%	50%
IG 30	Unity PF	-	61.854	30.958	16.272	9.811	6.447	4.078
	95% PF	-	49.986	31.22	15.904	9.406	5.864	4.168
PV A1	Unity PF	139.661	34.563	31.256	30.643	30.099	29.564	29.040
	85% PF	133.637	24.951	25.114	25.474	25.838	26.208	26.583
PV A2	Unity PF	82.839	39.982	33.001	31.304	30.507	29.742	28.997
	85% PF	297.062	22.941	23.362	24.288	25.252	26.254	27.296
PV A3	Unity PF	67.220	49.670	39.562	31.931	29.899	29.247	28.935
	85% PF	79.478	27.288	25.068	25.363	25.742	26.128	26.519
PV A4	Unity PF	68.023	49.848	39.466	31.717	29.689	29.046	28.739
	85% PF	85.273	26.939	24.830	25.148	25.536	25.930	26.330

Based on Table 9, the magnitude of THD_i is very high when the inverter is working under the nominal operation value of relative power. A low relative power means a low irradiance level. Therefore, the inverters absorb a significant amount of reactive power, which affects the magnitude of the harmonics current [26]. The result of past research shows that when inverters are working on high relative power, the magnitude of THD_i tends to get smaller both in 100% and 95% power factors. However, our research results show a different pattern, where inverters operating on 85% power factor tend to have increasing THD_i. In comparison, ones on 100% power factor tend to have decreasing THD_i. This discrepancy is caused by differences between the inverter's manufacturer or characteristics. The tendency of THD_i to increase when relative power rises is caused by the high irradiance level, which makes the inverters generate high reactive power. A high reactive power injected into the system means the amount of switching inside the components of the inverter is also high [20]. The higher the relative power of a non-unity power factor inverter, the magnitude of individual harmonic distortion (IHD) on low orders will also increase [22]. Figure 9 shows the harmonics order spectrum at 5% relative power and 100% PF as shown in Figure 9(a) 50% relative power and 100% PF as shown in Figure 9(b), 5% relative power and 85% PF as shown in Figure 9(c), 50% relative power 85% and PF Figure 9(d).

3.3. The effect of harmonics on system losses

Harmonics have a negative impact on the grid. The effect of harmonics on a distribution feeder can cause a power loss of up to 18% of the power absorbed by the load. In such a case, the THD in the current greatly influences the harmonics-induced losses. Figure 10 shows that power losses in cable B as shown in Figure 10(a) and cable F as shown in Figure 10(b) are greater at 100% power factor than at 85% power factor. This happens because inverters working at 85% power factor produce reactive power that acts as a reactive power compensator in the system [27]. Based on the modified grid code IEEE 1547a-2014, reactive power compensation by PV injection can regulate the voltage in the system and reduce system losses. This means that power losses in the cables can be reduced by injecting reactive power generated by the inverters, which also confirms the result of past research [28]. Harmonics-induced and fundamental power losses on both cable at 85% and 100% power factor can be seen in Table 10.

Irradiance received by the PV has a significant effect on cable power loss. Irradiance level is proportional to the active and reactive power generated. Past research has explained that a low irradiance level will affect the generation power factor, affecting the power losses in the cables. Therefore, the lower the irradiance level, the higher the power losses in the system or cables [29].

In the system used for our simulation, the power grid acts as a swing or reference to supply the demand that the distributed energy resources cannot. If the irradiance is low, the PV arrays' power output is reduced, meaning the grid has to supply more active and reactive power to meet the power demand. If the grid provides more power, there will be more power losses in the transformers and transmission lines, which means the overall system losses will also increase.

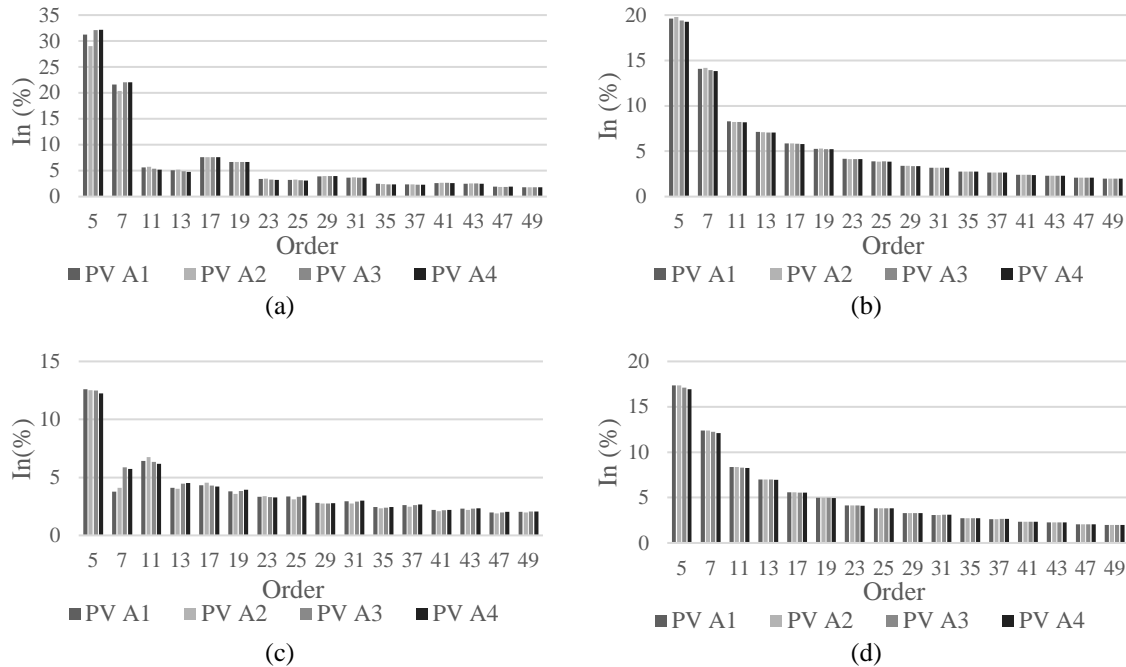


Figure 9. Harmonics spectrum (a) 5% relative power 100% PF, (b) 50% relative power 100% PF, (c) 5% relative power 85% PF, and (d) 50% relative power 85% PF

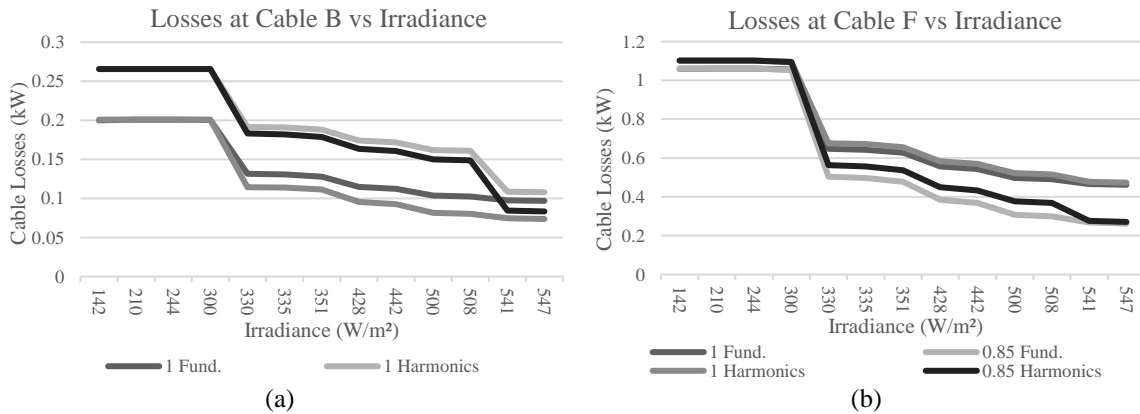


Figure 10. The effect of harmonics on losses at (a) cable B and (b) cable F

3.4. The effect of harmonics on transformer losses

High harmonics content in the system is unwanted because it is considered a disturbance. The distortion caused by high harmonic orders could lead to higher system losses, one of which is due to copper losses in transformers. Distribution transformers with nonlinear loads will increase the harmonics-induced power losses. Figure 11 shows that power losses in transformers 6 as shown in Figure 11(a) and transformers 4 as shown in Figure 11(b) are more significant at 100% power factor than at 85% power factor. This happens because inverters working at 85% power factor produce reactive power that acts as a reactive power compensator in the system [30]. Harmonics-induced and fundamental power losses on both transformers at 85% and 100% power factor can be seen in Table 11.

Table 10. The effect of harmonics on cable losses in kW

Irradiance (W/m ²)	Cable B				Cable F			
	Fundamental		Harmonics		Fundamental		Harmonics	
	100% PF	85% PF	100% PF	85% PF	100% PF	85% PF	100% PF	85% PF
142	0.1998	0.2009	0.2657	0.2657	1.0598	1.0608	1.1018	1.1018
210	0.2009	0.2009	0.2657	0.2657	1.0608	1.0608	1.1018	1.1018
244	0.2009	0.2009	0.2657	0.2657	1.0608	1.0608	1.1018	1.1018
300	0.2004	0.2009	0.2657	0.2657	1.0555	1.0523	1.0953	1.0942
330	0.1314	0.1143	0.1914	0.1832	0.6475	0.5036	0.6762	0.5627
335	0.1305	0.1139	0.1909	0.1821	0.6425	0.4977	0.6719	0.5573
351	0.1280	0.1115	0.1883	0.1786	0.6276	0.4782	0.6559	0.5373
428	0.1147	0.0954	0.1741	0.1633	0.5565	0.3849	0.5832	0.4492
442	0.1123	0.0925	0.1716	0.1605	0.5442	0.3689	0.5705	0.4340
500	0.1037	0.0816	0.1619	0.1502	0.4970	0.3074	0.5230	0.3765
508	0.1026	0.0803	0.1609	0.1488	0.4912	0.3000	0.5162	0.3689
541	0.0977	0.0746	0.1087	0.0844	0.4667	0.2679	0.4774	0.2766
547	0.0969	0.0737	0.1080	0.0833	0.4625	0.2625	0.4731	0.2711

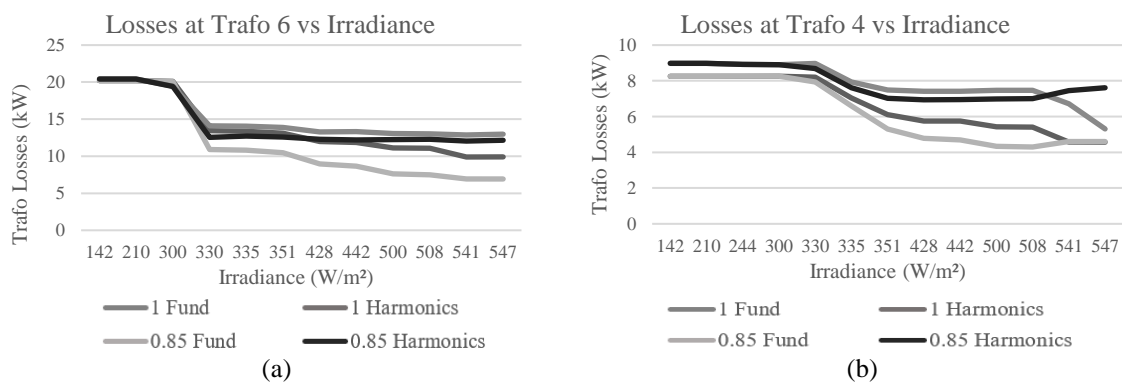


Figure 11. The effect of harmonics on losses at (a) transformer 6 and (b) transformer 4

Table 11. The effect of harmonics on transformer losses in kW

Irradiance (W/m ²)	Trafo 4				Trafo 6			
	Fundamental		Harmonics		Fundamental		Harmonics	
	100% PF	85% PF	100% PF	85% PF	100% PF	85% PF	100% PF	85% PF
0,09	8.254	8.254	8.98	8.98	20.196	20.196	20.42	20.42
210	8.254	8.254	8.98	8.98	20.196	20.196	20.42	20.42
244	8.254	8.253	8.913	8.916	20.195	20.195	20.405	20.405
300	8.253	8.252	8.912	8.911	20.09	20.054	19.442	19.41
330	8.2	7.93	8.974	8.694	13.462	10.92	14.107	12.543
335	7.038	6.59	7.941	7.691	13.38	10.816	14.049	12.723
351	6.118	5.302	7.491	7.024	13.126	10.467	13.888	12.578
428	5.744	4.775	7.425	6.939	11.978	8.946	13.297	12.285
442	5.744	4.693	7.419	6.952	11.859	8.644	13.305	12.203
500	5.435	4.344	7.463	6.993	11.099	7.622	13.058	12.261
508	5.403	4.3	7.476	7.006	11.077	7.491	13.042	12.286
541	4.576	4.602	6.721	7.461	9.896	6.931	12.869	12.044
547	4.577	4.606	5.309	7.613	9.897	6.935	12.989	12.137

4. CONCLUSION

On-grid PV systems with inverters working at 85% power factor cause a lower THD_i value than the system with a unity power factor. However, with the system set on 85% power factor, the THD_i value increases slowly as the irradiance increases. This differs from the system that runs at 100% power factor, in which the value of THD_i will decrease gradually. This is caused by the increasing number of switching of the inverters' components. In turn, this will cause the distortion to be bigger as irradiance increases in 85% power factor, which significantly increases IHD_i on the 5th order. Meanwhile, the THD_v value increases with 85% power factor and unity power factor as the irradiance increases. However, the THD_v value is higher at 85% power factor system than those at 100% power factor since there is more reactive power compensation if the irradiance increases. Relative power changes in the on-grid PV system cause the magnitude of the harmonic in the system to be dynamic, which will cause the losses to fluctuate on both electric lines and transformers. When the

irradiance increases, the losses on lines decrease. This is caused by less energy supplied from the grid, reducing the system losses and transformers losses. This condition applies when inverters operate on 85% power factor in which the network and transformers have smaller losses value than the unity power factor. Therefore, inverters with an 85% power factor have increased harmonics proportional to their irradiance level, so losses will slightly increase. From the case above, designing a system with power quality in mind is vital, especially to anticipate harmonics conditions and their effects on network losses. Furthermore, active or passive filters could be useful in a system with a high level of harmonics distortion. This research can describe harmonics conditions and their effects on network losses on the on-grid PV-integrated system when irradiance varies.

ACKNOWLEDGEMENTS

Completing this research is impossible without the support of other individuals or institutions. The researchers want to thank the Directorate of Research and Social Service of Sepuluh Nopember Institute of Technology, which provides the funding for this research, and the Power System Simulation Laboratory, which provides the facility and helps in completing this research.

REFERENCES

- [1] S. Kouro, J. I. Leon, D. Vinnikov, and L. G. Franquelo, "Grid-connected Photovoltaic systems: An overview of recent research and emerging PV converter technology," *IEEE Industrial Electronics Magazine*, vol. 9, no. 1, pp. 47–61, Mar. 2015, doi: 10.1109/MIE.2014.2376976.
- [2] A. Elkholy, "Harmonics assessment and mathematical modeling of power quality parameters for low voltage grid connected photovoltaic systems," *Solar Energy*, vol. 183, pp. 315–326, 2019, doi: 10.1016/j.solener.2019.03.009.
- [3] M. H. Rashid, *Power electronics*. Academic Press Series in Engineering, 2001.
- [4] D. Pejovski, K. Najdenkoski, and M. Dugalovski, "Impact of different harmonic loads on distribution transformers," *Procedia Engineering*, vol. 202, pp. 76–87, 2017, doi: 10.1016/j.proeng.2017.09.696.
- [5] D. Baimel, "Implementation of DQ0 control methods in high power electronics devices for renewable energy sources, energy storage and FACTS," *Sustainable Energy, Grids and Networks*, vol. 18, Jun. 2019, doi: 10.1016/j.segan.2019.100218.
- [6] G. Osma-Pinto, M. García-Rodríguez, J. Moreno-Vargas, and C. Duarte-Gualdrón, "Impact evaluation of grid-connected PV systems on PQ parameters by comparative analysis based on inferential statistics," *Energies*, vol. 13, no. 7, Apr. 2020, doi: 10.3390/en13071668.
- [7] K. B. Nagasai and T. R. Jyothsna, "Harmonic analysis and application of PWM techniques for three phase inverter," *International Research Journal of Engineering and Technology (IRJET)*, vol. 3, no. 7, pp. 1228–1233, 2016.
- [8] I. Gunnarsdottir, B. Davidsdottir, E. Worrell, and S. Sigurgeirsdottir, "Indicators for sustainable energy development: An Icelandic case study," *Energy Policy*, vol. 164, 2022, doi: 10.1016/j.enpol.2022.112926.
- [9] M. Bajaj and A. K. Singh, "Optimal design of passive power filter for enhancing the harmonic-constrained hosting capacity of renewable DG systems," *Computers and Electrical Engineering*, vol. 97, Jan. 2022, doi: 10.1016/j.compeleceng.2021.107646.
- [10] S. S. Parihar and N. Malik, "Analysing the impact of optimally allocated solar PV-based DG in harmonics polluted distribution network," *Sustainable Energy Technologies and Assessments*, vol. 49, Feb. 2022, doi: 10.1016/j.seta.2021.101784.
- [11] B. Bayer, P. Matschoss, H. Thomas, and A. Marian, "The German experience with integrating photovoltaic systems into the low-voltage grids," *Renewable Energy*, vol. 119, pp. 129–141, Apr. 2018, doi: 10.1016/j.renene.2017.11.045.
- [12] W. M. Grady and R. J. Gilleskie, "Harmonics and how they relate to power factor," in *Proceedings of the EPIR Power Quality Issues and Opportunities Conference. November, 1993*, pp. 1–8.
- [13] G. A. Rampinelli, F. P. Gasparin, A. J. Bühler, A. Krenzinger, and F. Chenlo Romero, "Assessment and mathematical modeling of energy quality parameters of grid connected photovoltaic inverters," *Renewable and Sustainable Energy Reviews*, vol. 52, pp. 133–141, 2015, doi: 10.1016/j.rser.2015.07.087.
- [14] G. Min, J. Qingren, and C. Weidong, "Analysis of the harmonics influence of urban rail transport load on Nanning power grid based on ETAP," in *2018 13th IEEE Conference on Industrial Electronics and Applications (ICIEA)*, 2018, pp. 594–599, doi: 10.1109/ICIEA.2018.8397785.
- [15] P. K. Bhatt, "Harmonics mitigated multi-objective energy optimization in PV integrated rural distribution network using modified TLBO algorithm," *Renewable Energy Focus*, vol. 40, pp. 13–22, Mar. 2022, doi: 10.1016/j.ref.2021.11.001.
- [16] A. Kalair, N. Abas, A. R. Kalair, Z. Saleem, and N. Khan, "Review of harmonic analysis, modeling and mitigation techniques," *Renewable and Sustainable Energy Reviews*, vol. 78, pp. 1152–1187, Oct. 2017, doi: 10.1016/j.rser.2017.04.121.
- [17] K. Kritsanasuwan, U. Leeton, and T. Kulworawanichpong, "Harmonic mitigation of AC electric railway power feeding system by using single-tuned passive filters," *Energy Reports*, vol. 8, pp. 1116–1124, Nov. 2022, doi: 10.1016/j.egy.2022.05.276.
- [18] *HARMONICS: A guide to supply harmonics and other low-frequency disturbance*. Nidec Control Techniques Limited. Registered Office: The Gro, Newtown, Powys SY16 3BE, 2020.
- [19] K. Shaarbafi, *Transformer modelling guide*. AESO-Alberta Electric System Operator, 2014.
- [20] W. Rahmouni, G. Bachir, and M. Aillerie, "Impact of reactive grid support strategies on power quality in photovoltaic systems," *Elektrotehniski Vestnik*, vol. 87, no. 5, pp. 243–250, 2020.
- [21] M. Talha, S. R. S. Raihan, and N. A. Rahim, "PV inverter with decoupled active and reactive power control to mitigate grid faults," *Renewable Energy*, vol. 162, pp. 877–892, 2020, doi: 10.1016/j.renene.2020.08.067.
- [22] K. P. Kontogiannis, G. A. Vokas, S. Nanou, and S. Papathanassiou, "Power quality field measurements on PV inverters," *Power*, vol. 2, no. 11, 2013.
- [23] R. R. A. Fortes, R. F. Buzo, and L. C. O. de Oliveira, "Harmonic distortion assessment in power distribution networks considering DC component injection from PV inverters," *Electric Power Systems Research*, vol. 188, Nov. 2020, doi: 10.1016/j.epr.2020.106521.
- [24] L. Xiong, M. Nour, and M. Shahin, "Harmonic analysis of high penetration level of Photovoltaic generation in distribution network and solution studies," in *2019 8th International Conference on Modeling Simulation and Applied Optimization (ICMSAO)*, Apr. 2019, pp. 1–5, doi: 10.1109/ICMSAO.2019.8880387.

- [25] S. M. Ahsan, H. A. Khan, A. Hussain, S. Tariq, and N. A. Zaffar, "Harmonic analysis of grid-connected solar PV systems with nonlinear household loads in low-voltage distribution networks," *Sustainability*, vol. 13, no. 7, Mar. 2021, doi: 10.3390/su13073709.
- [26] A. Chidurala, T. K. Saha, N. Mithulananthan, and R. C. Bansal, "Harmonic emissions in grid connected PV systems: A case study on a large scale rooftop PV site," in *2014 IEEE PES General Meeting | Conference & Exposition*, Jul. 2014, pp. 1–5, doi: 10.1109/PESGM.2014.6939147.
- [27] O. Gandhi, C. Rodriguez-Gallegos, T. Reindl, and D. Srinivasan, "Competitiveness of PV inverter as a reactive power compensator considering inverter lifetime reduction," *Energy Procedia*, vol. 150, pp. 74–82, 2018.
- [28] A. Das, A. Gupta, S. R. Choudhury, and S. Anand, "Adaptive reactive power injection by solar PV inverter to minimize tap changes and line losses," in *2016 National Power Systems Conference (NPSC)*, 2016, pp. 1–6, doi: 10.1109/NPSC.2016.7858955.
- [29] S. Adak and H. Cangi, "The quality problems in low irradiance at grid connected PV solar system," *Research Square*, no. 1–10, 2022.
- [30] S. Vlahinić, D. Franković, V. Komen, and A. Antonić, "Reactive power compensation with PV inverters for system loss reduction," *Energies*, vol. 12, no. 21, 2019, doi: 10.3390/en12214062.

BIOGRAPHIES OF AUTHORS



Ontoseno Penangsang    received the bachelor degree in electrical engineering from Sepuluh Nopember Institute of Technology, Surabaya, Indonesia, in 1974 and the M.Sc. as well as Ph.D. degrees in power system analysis from the University of Wisconsin-Madison, Wisconsin, USA, in 1979 and 1983, respectively. Currently, he is a Professor at the Department of Electrical Engineering, Sepuluh Nopember Institute of Technology. He is also one of the researchers at the Power System Simulation Laboratory, Department of Electrical Engineering, Sepuluh Nopember Institute of Technology. His research interests include power system simulation and analysis and power quality. He can be contacted at email: zenno379@gmail.com.



Rony Seto Wibowo    received the bachelor degree in electrical engineering from Sepuluh Nopember Institute of Technology, Surabaya, Indonesia, in 1999. He holds a master's degree in electrical engineering from Bandung Institute of Technology, Bandung, Indonesia, and a Dr. Eng degree in electrical power and energy system from Hiroshima University, Japan. He is currently the Head of the Power System Simulation Laboratory at the Department of Electrical Engineering, Sepuluh Nopember Institute of Technology. His research interests include power system operation, power system planning, renewable energy, and power system economics. He can be contacted at email: ronseto@ee.its.ac.id.



Ni Ketut Aryani    received bachelor, master, and doctoral degrees in Electrical Engineering from Sepuluh Nopember Institute of Technology, Surabaya, Indonesia, in 1990, 2007, and 2018, respectively. She is currently a lecturer at the Department of Electrical Engineering, Sepuluh Nopember Institute of Technology, Surabaya, Indonesia. Her research interests include power system operation, power system economics, and power quality. She can be contacted at email ketut.aryani@gmail.com.



Mario Dwi Prasetyo    is a student at Sepuluh Nopember Institute of Technology, Surabaya, Indonesia. Currently, he is pursuing a bachelor's degree in electrical engineering at Sepuluh Nopember Institute of Technology. He is also an assistant at Power System Simulation Laboratory at the Department of Electrical Engineering, Sepuluh Nopember Institute of Technology. He can be contacted at email dwimario874@gmail.com.



Marcel Nicky Arianto    is a student at Sepuluh Nopember Institute of Technology, Surabaya, Indonesia. Currently, he is pursuing a bachelor's degree in electrical engineering at Sepuluh Nopember Institute of Technology. He is also an assistant at Power System Simulation Laboratory at the Department of Electrical Engineering, Sepuluh Nopember Institute of Technology. He can be contacted at email Marcelnicky27@gmail.com.



Aulia Amjad Lutfi    is a student at Sepuluh Nopember Institute of Technology, Surabaya, Indonesia. Currently, he is pursuing a bachelor's degree in electrical engineering at Sepuluh Nopember Institute of Technology. He is also an assistant at Power System Simulation Laboratory at the Department of Electrical Engineering, Sepuluh Nopember Institute of Technology. He can be contacted at email: amjadlutfi@gmail.com.